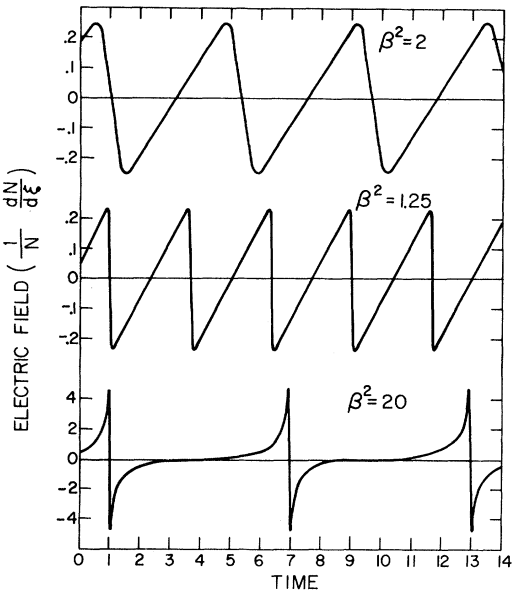

FIG. 3. Numerical solution of the electric field in a nonlinear electrostatic cyclotron wave.

cles which are not considered in our analysis. The nonlinear waves in Fig. 1 do not have a larger electric-field-potential amplitude than the waves having a sinusoidal form. This is consistent since it is the ratio of amplitude to the plasma temperature $e\varphi/kT$ that is important and not the absolute amplitude (φ).

The Fourier transform of a sawtooth or spiky wave has an infinite number of harmonics. The phase and amplitude of the harmonics are determined by the form of the original wave. Harmonics can also be generated linearly in the Vlasov theory of the electrostatic ion cyclotron wave. However, in the absence of nonlinear coupling between the harmonics, such waves would be expected to have relative phases and amplitudes different from those necessary to produce sawtooth or spiky solutions.

We have shown that a simple solution of the equations characterizing electrostatic ion cyclotron wave reproduces the essential features of the observed wave form. A more complete analysis would need to include, among other things, the effects of several traveling waves, arbitrary initial conditions, resonant particles, the linear generation of the higher-order harmonics, and other nonlinear effects.[8]

This research was supported in part by the U. S. Office of Naval Research under Contract No. NOOO14-75-C-0294.

[1]N. D'Angelo and R. W. Motley, Phys. Fluids 5, 633 (1963).

[2]W. E. Drummond and M. N. Rosenbluth, Phys. Fluids 5, 1507 (1962).

[3]J. M. Kindel and C. F. Kennel, J. Geophys. Res. 76, 3055 (1971).

[4]F. S. Mozer, C. W. Carlson, M. K. Hudson, R. B. Torbert, B. Parady, J. Yatteau, and M. C. Kelley, Phys. Rev. Lett. 38, 292 (1977); P. M. Kintner, M. C. Kelley, and F. S. Mozer, Geophys. Res. Lett. 5, 139 (1978).

[5]P. M. Kintner, M. C. Kelley, R. D. Sharp, A. G. Ghielmetti, M. Temerin, C. Cattell, and P. Mizera, to be published.

[6]P. K. Chatervedi, Phys. Fluids 19, 1064 (1976).

[7]L. D. Landau and E. M. Lifshitz, *Fluid Mechanics* (Pergamon, New York, 1959).

[8]J. R. Myra and C. S. Liu, Phys. Rev. Lett. 43, 861 (1979).

Effect of Electrostatic Fields on Charged Reaction Products in Six-Beam Symmetrical Implosion Experiments

Y. Gazit,[a] J. Delettrez, T. C. Bristow, A. Entenberg, and J. Soures
Laboratory for Laser Energetics, University of Rochester, Rochester, New York 14623
(Received 27 June 1979)

Alpha and proton reaction product spectra have been measured in exploding pusher experiments on the symmetrical illumination six-beam ZETA laser system (Nd-doped phosphate glass). DT ion temperatures and positive energy shifts for α particles and protons were obtained for experiments with incident on-target power between 1 and 2.5 TW. Time-averaged electrostatic potentials have been measured up to 330 kV.

Symmetrical exploding pusher experiments have been conducted on the six-beam ZETA laser system of the Laboratory for Laser Energetics at the University of Rochester.[1] In these experiments 70-psec pulses [full width at half maximum (FWHM)] with a peak power from 1 to 2.5 Tw [in-

tensity (from 3 to 8)$\times 10^{15}$ W/cm^2] at 1.054 μm were focused on thin-wall glass microballoons (0.6 to 1.3 μm) filled with 2 and 4 mg/cm^3 of equimolar DT. The α-particle and proton energy spectra were measured in order to obtain the DT ion temperature. DT ion temperatures ranging from 2.0 to 4.0 keV were obtained from the broadening of the α-particle spectrum and from the ratio of the α and proton yield. Comparisons were made between experimental results and those calculated by the one-dimensional Lagrangian hydrodynamic code LILAC.[2]

Measurements of charged fusion products have been previously reported by three laboratories.[3] Positive energy shifts from α's and protons in long pulses have been observed at Lawrence Livermore Laboratory.[4] In this paper we report the observation of nonthermal α-particle spectral broadening and the measurement of α-particle spectral broadening and the measurement of α-particle and proton positive energy shifts. These effects can be attributed to a time-varying electrostatic potential which is created during the laser pulse.

The α particles from the reaction D(T,α)n and the protons from the reaction D(D,T)p were measured with a time-of-flight spectrometer with a flight path of 277 cm.[5] The detector consists of NE111 scintillator, 0.178 mm thick, coupled to an Amperex XP2020 photomultiplier tube. The acceptance solid angle is 1.26×10^{-3} sr. The uncertainty in the mean α energy is estimated to be $\pm$ 70 keV and the width of the instrumental response for a single α particle is 4 nsec. The latter is equivalent to an instrumental broadening of 130 keV for an α energy of 3.52 MeV. Figure 1 shows sample traces of the α particle and proton energy spectra.

The DT ion temperature is estimated in two ways: from the thermal broadening of the α particle spectrum[6] and from the ratio of the α particle and proton yields. The FWHM, ΔE_α, of the α-particle energy spectrum is calculated by subtracting in quadrature the instrumental broadening, $\Delta E_{\rm inst}$, and that due to the time-varying collisional energy losses in the DT fuel and tamper (glass shell), ΔE_{ti}, from the measured width, $\Delta E_{\rm obs}$: $\Delta E_\alpha = (\Delta E_{\rm obs}{}^2 - \Delta E_{\rm inst}{}^2 - \Delta E_{ti}{}^2)^{1/2}$. Estimates of ΔE_{ti} are of the order of 140 keV for thick-wall (1.2 μm) and 60 keV for thin-wall (0.8-μm) targets. These estimates are obtained from the code LILAC[2] in which the reaction products are transported by ray tracing over several angular directions using a standard energy-loss formula[7] corrected for Thomas-Fermi effects. The ion temperature is computed from $\theta_i = (\Delta E_\alpha/177)^2$ with θ_i and ΔE_α in keV.[6]

A summary of the ion-temperature results in

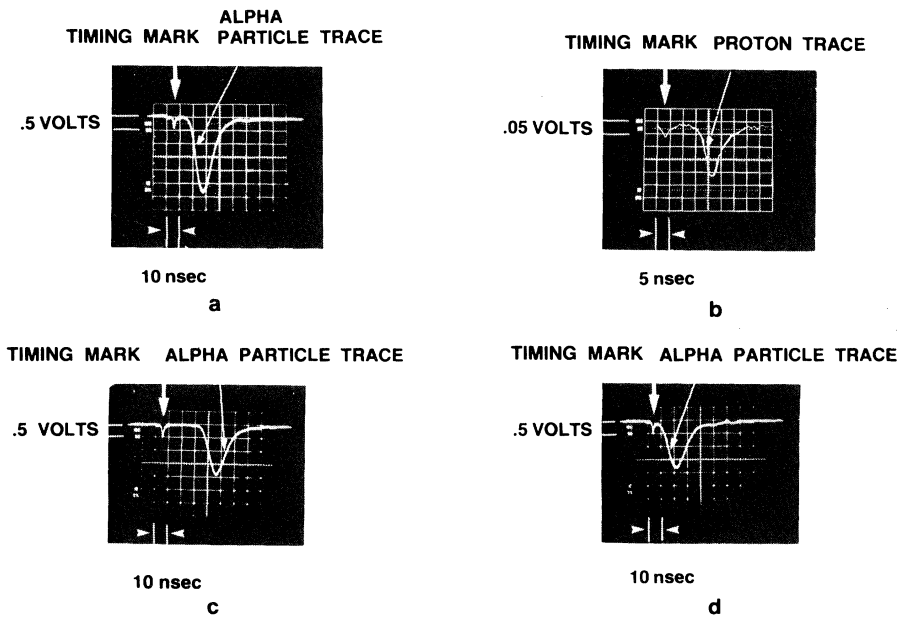

FIG. 1. Oscilloscope traces from the time-of-flight spectrometer: (a) α-particle trace with mean energy of 3.17 MeV from shot 1917; (b) proton trace from shot 1917 with mean energy of 2.92 MeV; (c), (d) α-particle traces from shots 1843 and 1801 with mean α energies of 3.08 and 3.80 MeV, respectively.

TABLE I. Summary of ion-temperature results. Temperatures: $\theta_i{}^a$ from spectral broadening, $\theta_i{}^b$ from ratio of yields, $\theta_i{}^c$ from LILAC. Uncertainties: ±0.07 MeV for E_α, ±15% for ΔE_α, ±30% for $\theta_i{}^a$, and ±40% for $\theta_i{}^b$.

Shot No.	Power (TW)	Diameter (μm)	Wall thickness (μm)	ϵ_a (J/ng)	Neutron yield (10^8)	$\bar{E}_\alpha$ (MeV)	ΔE_α (keV)	$\theta_i{}^a$ (keV)	$\theta_i{}^b$ (keV)	$\theta_i{}^c$ (keV)	Neutron yield[a] (10^8)
1735	1.3	119	1.1	0.17	2.3	3.10	316	3.2	3.2	2.7	1.7
1801	1.3	73	0.8	0.79	1.5	3.80	554	9.8	3.0	3.9	1.7
1843	1.1	113	1.1	0.20	1.5	3.08	350	3.9	2.5	3.8	1.2
1917	2.2	111	1.2	0.26	3.0	3.17	358	4.0	3.6	3.7	2.8

[a]As obtained from LILAC.

Table I includes shot parameters, experimental results, and the results of LILAC simulations. For the three shots with low specific absorbed energy (ϵ_a is the ratio of absorbed energy to target mass), there is a negative α energy shift (of $\bar{E}_\alpha$, the mean α energy, from 3.52 MeV) and good overall agreement between the ion temperatures obtained by the two methods and that estimated from the code-calculated α-particle spectrum. In shot 1801, characterized by a high ϵ_a, there is a positive energy shift and an additional spectral broadening of nonthermal origin. The latter is inferred from the fact that the ion temperatures from yield ratios and code prediction were 3 and 3.9 keV, respectively, while the ion temperature from the α spectral width would imply 9.8 keV. Moreover, this combination of a positive energy shift and similarly enhanced spectral broadening has been observed in two additional shots (Table II) with relatively high ϵ_a.

A monotonically increasing dependence of α energy shifts on ϵ_a is shown in Fig. 2 where the mean α energy is plotted versus ϵ_a. As shown in the figure, the code LILAC (which corrects for collisional losses in the tamper) is only able to simulate the negative energy shifts for ϵ_a less than 0.4 J/ng. To explain the positive shifts which occur for ϵ_a greater than 0.55 J/ng, there must be an electrostatic potential difference, $\Delta\varphi$, which accelerates the α particles.

The minimum value of the potential difference experienced by each particle may be estimated directly from the measured α and proton energy shifts: $\Delta\varphi_{\min}{}^{\alpha}(2e)^{-1}(\delta E)_M{}^{\alpha}$ and $\Delta\varphi_{\min}{}^{p}=e^{-1}(\delta E)_M{}^{p}$. An estimate of the entire potential difference, $\Delta\varphi$, can be made if the measured energy shift is first corrected by the collisional energy loss, $(\delta E)_{\text{col}}{}^{\text{code}}$, (calculated by LILAC) in the core and tamper. Minimum potential values between 140 and 265 kV and code-corrected estimates between 215 and 330 kV are shown in Table II for three shots with high ϵ_a.

Insight into the temporal behavior of the potential is provided by Fig. 3 which shows two time histories. For high ϵ_a, the majority of α's are produced between the peak of the laser pulse and approximately one pulse width (FWHM) after the peak. As ϵ_a decreases, the implosion velocity also decreases and α-particle production occurs more than a pulse width after the peak. The fact that positive energy shifts and enhanced spectral broadening are only present in the shots with

TABLE II. Energy shift contributions. Uncertainties: ±70 keV for $(\delta E)_M{}^{\alpha}$, ±100 keV for $(\delta E)_M{}^{p}$; ±50 kV for $\Delta\varphi^{\alpha}$, ±100 kV for $\Delta\varphi^{p}$.

Shot No.	Power (TW)	Diameter (μm)	Wall thickness (μm)	ϵ_α (J/ng)	Neutron yield (10^8)	$(\delta E)_M$ (keV)	$(\delta E)_{\text{col}}{}^{\text{code}}$ (keV)	$\Delta\varphi_{\min}$ (kV)	$\Delta\varphi$ (kV)
1736	1.0	67	0.8	1.1	1.4	α: 430	-200	215	315
						p: 265	-65	265	330
1800	1.3	68	0.8	0.84	1.5	α: 330	-170	165	250
						p: 236	-60	236	296
1801	1.3	73	0.8	0.79	1.5	α: 279	-150	140	215
						p: 207	-50	207	257

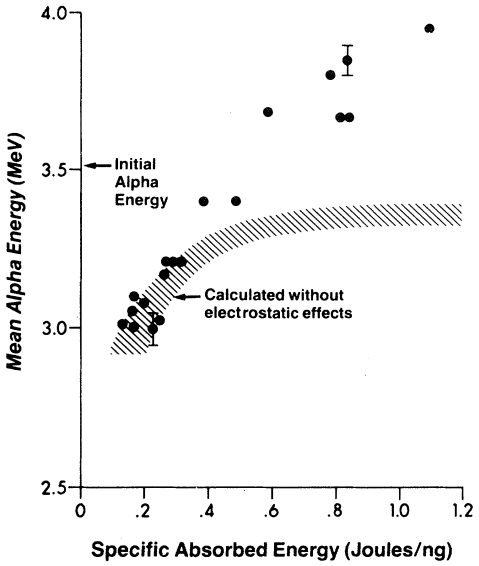

FIG. 2. Scaling of α-particle mean energy with specific absorbed energy. Included is the region of calculations without electrostatic effects. Experimental points show a positive energy shift above the initial value of 3.52 MeV.

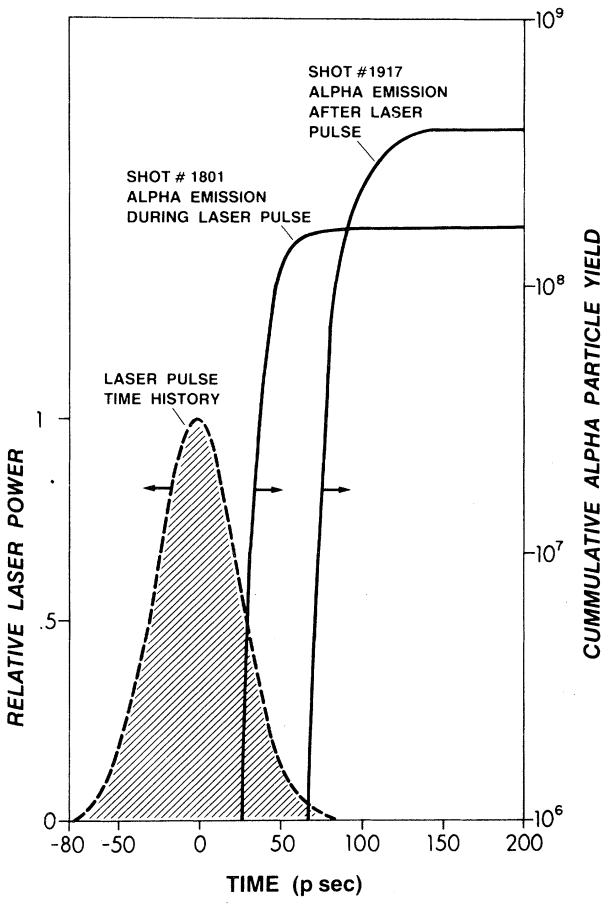

FIG. 3. α-production time history relative to the laser pulse calculated by the code LILAC: high specific absorbed energy (0.79 J/ng) for shot 1801; low specific absorbed energy (0.26 J/ng) for shot 1917.

higher ϵ_a suggests that the electrostatic potential is created during, and decays shortly after, the laser pulse. α's and protons produced a significant time after the laser pulse will not experience the full potential difference.

The electrostatic potential results from the presence of laser-produced hot electrons. These electrons, whose temperature follows the laser pulse intensity,[8] are responsible for the quasi-neutral and sheath potentials of the corona.[9] There is also a vacuum potential created by electrons which escape, thereby leaving the pellet positively charged.[10] The potential decays after the laser pulse because of the cessation of hot-electron production, the cooling of hot electrons during expansion, and neutralizing currents from the stalk.[11]

In conclusion, the existence of an electrostatic potential has been inferred from positive energy shifts and nonthermal spectral broadening. Measurement and comparison with code-calculated time histories suggest that this potential is created during and decays shortly after the laser pulse.

The authors would like to thank S. Kacenjar for his assistance with solid-angle calculations, S. Skupsky for the use of his reaction-product transport code, and E. Williams, M. True, L. Goldman, J. Geiger, and A. Bennish for helpful discussions. This work was partially supported by Exxon Research and Engineering Company, General Electric Company, Northeast Utilities, Empire State Electric Energy Research Corporation, and New York State Energy Research and Development Administration.

---

[a]Permanent address: Soreq Nuclear Research Center, Yavne 70600, Israel.

[1]J. Bunkenburg and W. Seka, in *Digest of Technical Papers, IEEE–Optical Society of America Conference on Laser Engineering and Applications, Washington, D.C., 1979* (IEEE, New York, 1979), p. 96.

[2]E. B. Goldman, Laboratory of Laser Energetics Report No. 16, 1973 (unpublished); J. Delettrez and E. B. Goldman, Laboratory of Laser Energetics Report No. 36, 1976 (unpublished).

[3]V. W. Slivinsky, H. G. Ahlstrom, K. S. Tiresell, J. Larsen, S. Glaros, G. Zimmermann, and H. Shay, Phys. Rev. Lett. 35, 1083 (1975); G. H. McCall and R. L. Morse, Laser Focus 10, 40 (1974); P. Campbell, G. Charatis, and G. Montry, Phys. Rev. Lett. 34, 74 (1975); G. H. McCall, T. H. Tan, and A. Williams, Bull. Am. Phys. Soc. 20, 1318 (1975); T. H. Tan, G. H. McCall, and A. Williams, Bull. Am. Phys. Soc. 20, 1318 (1975); R. R. Goforth, F. J. Mayer, H. Brysk, and R. A. Cover, J. Appl. Phys. 47, 4850 (1976).

[4]M. J. Boyle *et al.*, Lawrence Livermore Laboratory Report No. UCRL-79779, 1977 (unpublished).

[5]Y. Gazit, Bull. Am. Phys. Soc. 23, 880 (1978).

[6]H. Brysk, Plasma Phys. 15, 611 (1973).

[7]C. Longmire, *Elementary Plasma Physics* (Wiley, New York, 1967), p. 202.

[8]P. H. Lee and M. D. Rosen, Phys. Rev. Lett. 42, 236 (1979).

[9]J. E. Crow, P. L. Auer, and J. E. Allen, J. Plasma Phys. 14, 65 (1975).

[10]J. S. Pearlman and G. Dahlbacka, Appl. Phys. Lett. 31, 414 (1977).

[11]R. F. Benjamin, G. H. McCall, and A. W. Ehler, Phys. Rev. Lett. 42, 890 (1979).

Resonance Photon Scattering from $^{15}N_2$ Monolayers Adsorbed on Grafoil

R. Moreh[a] and O. Shahal

Nuclear Research Center, Negev, Beer Sheva, Israel, and Ben-Gurion, University of the Negev, Beer Sheva, Israel

(Received 17 September 1979)

Nuclear resonance scattering of photons from ^{15}N has been used to study the orientation of the N_2 molecular axis with respect to the adsorbing Grafoil plane. At 78 °K, and around 1 monolayer coverage, the N_2 molecules were found to be aligned preferentially parallel to the plane of graphite. At lower coverage, of ~0.8 monolayer, some parallel orientation is retained while at a coverage of 1.5 monolayers no preferred orientation was obtained.

The nuclear-resonance-scattering cross section of 6.324-MeV photons from $^{15}N_2$ molecules adsorbed on Grafoil has been measured as a function of the coverage. Film thicknesses of N_2 ranging from ~0.8 to ~1.5 monolayers have been used. A strong dependence of the photon scattering intensity on the angle between the c axis of the Grafoil and the direction of the photon beam was observed. This is interpreted as due to the particular orientation of the adsorbed N_2 molecule with respect to the c axis of graphite.

The present technique is entirely new and can be applied to the adsorption of $^{15}N_2$ gas only as it depends on the fact that the 6.324-MeV level in ^{15}N is photoexcited[1,2] by a chance overlap (to within ~30 eV) with one of the γ lines of the reaction $Cr(n, \gamma)$. The nuclear-scattering cross section σ_s is so high (~1.4 b) and the background is so low that detectable scattered signals are obtained even from targets containing ~10 mg of ^{15}N. In addition, since a resonance-scattering process is involved the graphite substrate is essentially transparent to the incident photon beam.

In a recent publication,[3] it was noted that σ_s is strongly dependent on the kinetic-energy component of the N atom (including that of its *zero-point* motion) along the photon-beam direction. This is because σ_s is determined by the overlap between the two Doppler-broadened shapes of the incident γ line and the resonance level. In fact, a one-to-one correspondence was established[3] between σ_s and the effective[4] temperature T_e of the N atom, where T_e gives a measure of the total kinetic energy of the N atom including that of its zero-point motion.

From the above it may be seen that σ_s would be highest when the axis of the linear $^{15}N_2$ molecule coincides with the γ-beam direction because of the increased kinetic energy of the N atom contributed by the *zero-point* vibrational energy of the N_2 molecule. Hence σ_s can be used as a very sensitive monitor of the angle between the line joining the diatomic N_2 molecule and the photon direction. In the present work we used this fact for studying the orientation of adsorbed $^{15}N_2$ molecules on partially oriented graphite foil known commercially as "Grafoil."

Experimentally, the photon beam is obtained from the (n, γ) reaction on some chromium disks placed along a tangential beam tube and near the core of the IRR-2 reactor.[1] The intensity of the 6.324-MeV γ line emitted by the reaction $^{53}Cr(n, \gamma)$ is relatively weak amounting to ~10^4 photons/cm^2 sec at the target position. The target consisted of variable amounts of enriched $^{15}N_2$ gas (99.3%) adsorbed on Grafoil. A total of 84 rec-

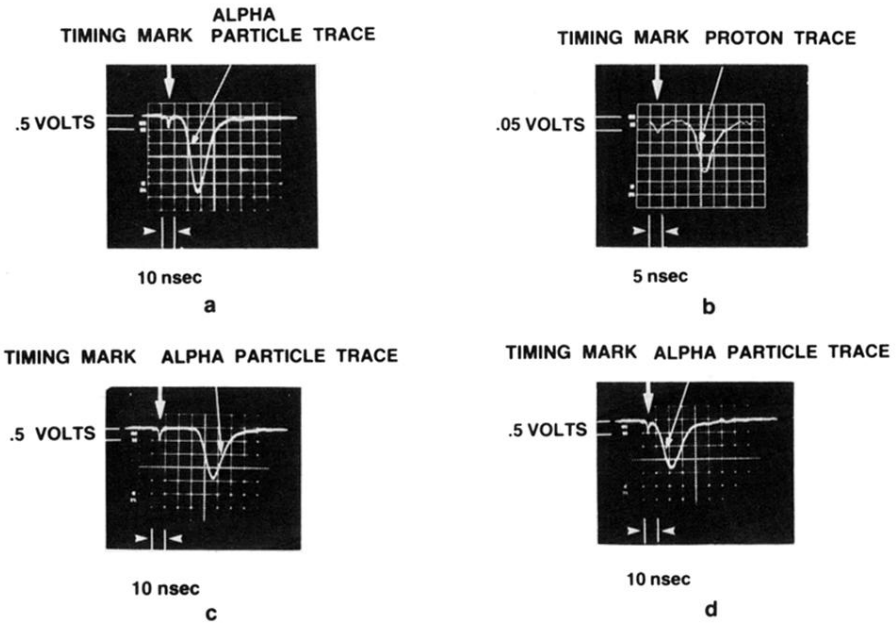

FIG. 1. Oscilloscope traces from the time-of-flight spectrometer: (a) α-particle trace with mean energy of 3.17 MeV from shot 1917; (b) proton trace from shot 1917 with mean energy of 2.92 MeV; (c), (d) α-particle traces from shots 1843 and 1801 with mean α energies of 3.08 and 3.80 MeV, respectively.